The Journal of Immunology

RESEARCH ARTICLE | JANUARY 17 2024

Neonatal CD8+ T Cells Resist Exhaustion during Chronic Infection

Viviana I. Maymí; ... et. al

J Immunol (2024) 212 (5): 834–843.
https://doi.org/10.4049/jimmunol.2300396

Neonatal CD8$^+$ T Cells Resist Exhaustion during Chronic Infection

Viviana I. Maymí,* Hongya Zhu,† Mason Jager,‡ Shawn Johnson,* Rodman Getchell,* James W. Casey,* Jennifer K. Grenier,§ E. John Wherry,¶ Norah L. Smith,* Andrew Grimson,† and Brian D. Rudd*

Chronic viral infections, such as HIV and hepatitis C virus, represent a major public health problem. Although it is well understood that neonates and adults respond differently to chronic viral infections, the underlying mechanisms remain unknown. In this study, we transferred neonatal and adult CD8$^+$ T cells into a mouse model of chronic infection (lymphocytic choriomeningitis virus clone 13) and dissected out the key cell-intrinsic differences that alter their ability to protect the host. Interestingly, we found that neonatal CD8$^+$ T cells preferentially became effector cells early in chronic infection compared with adult CD8$^+$ T cells and expressed higher levels of genes associated with cell migration and effector cell differentiation. During the chronic phase of infection, the neonatal cells retained more immune functionality and expressed lower levels of surface markers and genes related to exhaustion. Because the neonatal cells protect from viral replication early in chronic infection, the altered differentiation trajectories of neonatal and adult CD8$^+$ T cells is functionally significant. Together, our work demonstrates how cell-intrinsic differences between neonatal and adult CD8$^+$ T cells influence key cell fate decisions during chronic infection. *The Journal of Immunology*, 2024, 212: 834–843.

Neonates are highly susceptible to infection and often generate incomplete immunity against viruses and bacteria (1–3). Because CD8$^+$ T cells play a critical role in protecting the host against pathogens, it is important to understand how neonatal CD8$^+$ T cells respond to infection differently than adult cells. Recent studies have indicated that neonatal and adult CD8$^+$ T cells are distinguished by their developmental origins, unique gene expression profiles, distinct chromatin landscapes, altered usage of metabolic programs, and different kinetics and phenotypes postinfection (4–7). Whereas neonatal CD8$^+$ T cells mount rapid responses to infection and give rise to short-lived effectors, adult CD8$^+$ T cells respond with slower kinetics but have an enhanced ability to form long-lived memory cells. These studies led to the new idea that neonatal CD8$^+$ T cells fail to form memory not because of an inability to respond to infection, but rather because they more quickly become terminally differentiated. However, nearly all of the work to date has been performed in the context of acute infection. Thus, an important and unanswered question is how cell-intrinsic differences alter the fates of neonatal and adult CD8$^+$ T cells during chronic infection.

During chronic infection, persistent TCR stimulation induces a hypofunctional state known as T cell exhaustion (8–10). Exhausted CD8$^+$ T cells express inhibitory receptors, such as PD-1 and Tim-3, and lose the ability to secrete cytokines and cytotoxic molecules in a hierarchical manner (11). Although these properties prevent exhausted CD8$^+$ T cells from clearing infection, they allow the cells to persist during chronic stages of infection without causing excessive immunopathology, which is beneficial to the host (12–14). T cell exhaustion has been targeted therapeutically with inhibitory checkpoint blockade, which restores immune functionality and has revolutionized our approach to treating patients with chronic infections and cancer (15–17). However, the lack of universal efficacy and the unpredictable nature of adverse events have highlighted the need to better understand why some CD8$^+$ T cells become more severely exhausted than others.

In the case of neonatal and adult CD8$^+$ T cells, what are the different possible outcomes following chronic infection? On the one hand, it is possible that neonatal CD8$^+$ T cells more rapidly become exhausted (or even deleted) because of their enhanced ability to respond to antigenic stimulation. Our previous work demonstrated that neonatal CD8$^+$ T cells possess a more effector-like transcriptome and chromatin landscape prior to stimulation (5). As a consequence, they are hard-wired to respond rapidly to infection, which may cause them to more quickly undergo clonal exhaustion. On the other hand, it is possible that adult CD8$^+$ T cells preferentially become exhausted because during acute infection, they give rise to less-differentiated (KLRG1^{lo}) effector cells, which are the source of exhausted cells during chronic infection (18, 19). The slower response to infection by adult cells may also provide them with the flexibility to acquire stable phenotypes (e.g., exhaustion) that allow them to persist during chronic infection.

*Department of Microbiology and Immunology, Cornell University, Ithaca, NY; †Department of Molecular Biology and Genetics, Cornell University, Ithaca, NY; ‡Department of Population Medicine and Diagnostic Sciences, Cornell University, Ithaca, NY; §Transcriptional Regulation and Expression Facility, Department of Biomedical Sciences, Cornell University, Ithaca, NY; and ¶Institute for Immunology and Immune Health and Department of Systems Pharmacology and Translational Therapeutics, University of Pennsylvania Perelman School of Medicine, Philadelphia, PA

ORCIDs: 0000-0002-1575-3510 (V.I.M.); 0000-0003-1751-1782 (H.Z.); 0000-0001-6036-9895 (M.J.); 0009-0008-6016-7837 (S.J.); 0000-0003-4063-4668 (R.G.); 0000-0002-7495-7660 (N.L.S.).

Received for publication June 12, 2023. Accepted for publication January 1, 2024.

This work was supported by National Institute of Allergy and Infectious Disease, National Institute of Health Grants R01AI105265 (to B.D.R.), R01AI0613 (to B.D.R. and A.G.), R01AI166433 (to A.G.), F30OD032097 (to V.I.M.), R01AI55577 (to E.J.W.), R01AI115712 (to E.J.W.), U19AI117950 (to E.J.W.), PO1AI108545 (to E.J.W.), and U19AI082630 (to E.J.W.); National Institute of Health, National Cancer Institute, Basic Research Laboratory Grant CA210944 (to E.J.W.); and funds from the Parker Institute for Cancer Immunotherapy (to E.J.W.).

Address correspondence and reprint requests to Dr. Brian D. Rudd, Department of Microbiology and Immunology, C5 147 VMC, Cornell University, Ithaca, NY 14853. E-mail address: bdr54@cornell.edu

The online version of this article contains supplemental material.

Abbreviations used in this article: CAR, chimeric Ag receptor; CPM, counts per million; dpi, d postinfection; LCMV, lymphocytic choriomeningitis virus.

https://doi.org/10.4049/jimmunol.2300396

To differentiate between these possibilities, we used transgenic P14 $CD8^+$ T cells from adult (8–12 wk old) or neonatal (5–7 d old) mice, and lymphocytic choriomeningitis virus (LCMV) clone 13 as a model of chronic infection. First, we focused on early stages of chronic infection and asked whether neonatal $CD8^+$ T cells are biased toward becoming short-lived effectors. Then, we shifted our focus to the chronic phase of infection and examined whether neonatal or adult $CD8^+$ T cells preferentially became exhausted. We also compared the ability of neonatal and adult $CD8^+$ T cells to limit viral replication and protect the host from disease during chronic infection. Collectively, our work revealed that cell-intrinsic differences in neonatal and adult $CD8^+$ T cells are key determinants of their fates at different stages of chronic infection, which has important implications for neonatal immunity and immunotherapy for chronic viruses and cancer alike.

Materials and Methods

Mice

P14 transgenic mice expressing an LCMV GP33-41-specific H-$2D^b$–restricted TCR were obtained from John Wherry (University of Pennsylvania) and back-crossed to commercially available Pep3BoyJ mice (B6.SJL-*Ptprc*^{a} *Pepc*^{b}/BoyJ) for at least two generations before use and then maintained in our colony. P14 transgenic mice were then crossed with commercially available congenic (B6.PL-*Thy1*^{a}/CyJ) and wild-type C57BL/6J mice (The Jackson Laboratory) for adoptive cotransfer experiments. The Pep3BoyJ mice (B6.SJL-*Ptprc*^{a} *Pepc*^{b}/BoyJ) and TCRαKO mice (B6.129S2-*Tcra*^{tm1Mom}/J) were purchased from The Jackson Laboratory and then maintained in our colony. Neonatal mice were used between 5 and 7 d of age, and adult mice were 8–12 wk old. Both female and male mice were used for the experiments, and all mice were maintained under specific-pathogen–free conditions at the Cornell University College of Veterinary Medicine, accredited by the American Association of Accreditation of Laboratory Animal Care. The experiments in this study were conducted with approval from the Institutional Animal Care and Use Committee at Cornell University.

Lymphocyte isolation

In brief, spleens and inguinal lymph nodes were mashed through 40-μm strainers to create single-cell suspensions, and then the spleens were magnetically enriched with CD8α microbeads (Miltenyi Biotec; catalog no. 130-117-044) per the manufacturer's instructions. For adoptive transfers, two rounds of magnetic enrichment were performed to maximize the purity of the transferred population. The lungs were collected in 2.5-mL RP-5 with 0.5 mg/ml collagenase I (Worthington, catalog no. LS004196) and 0.02 mg/ml DNAse (Sigma–Aldrich catalog no. D4513) in gentleMACS C Tubes (Miltenyi Biotec) and then dissociated on the gentleMACS Octo Dissociator with Heaters program 37C_m_LDK_1 for 30 min under continuous rotation (Miltenyi Biotec). Single-cell suspensions were filtered through 70-μm filters, RBCs were lysed with ammonium-chloride-potassium lysis buffer for 5 min at room temperature, and then the suspension was filtered again through 40-μm filters. Livers were collected in 3 mL of RP-5 in gentleMACS C tubes (Miltenyi Biotec), dissociated on the gentleMACS Octo Dissociator with Heaters program m_liver_03 and m_liver_04, and then run through a Percoll gradient to enrich for lymphocytes. RBCs were lysed as with the lung, and single-cell suspensions were filtered through 40-μm filters.

Adoptive transfers

For adoptive cotransfers, 2×10^3 $CD8^+$ T cells were isolated from the spleens of congenically marked neonatal and adult P14 transgenic mice and then cotransferred into the same Pep3BoyJ recipient mice in 100 μl of sterile PBS via retro-orbital injection. For single transfers, 4×10^3 adult or neonatal P14 transgenic $CD8^+$ T cells were injected into separate Pep3BoyJ mice. For TCRαKO experiments, 1×10^4 adult and neonatal P14 transgenic $CD8^+$ T cells were injected into separate mice. For cytotoxicity assays, 5×10^4 to 1×10^5 adult and neonatal P14 transgenic $CD8^+$ T cells were injected into separate mice.

Infections

LCMV clone 13 was generously provided by John Wherry (University of Pennsylvania). One day after adoptive transfer, 2×10^6 PFU LCMV clone 13 was suspended in 100 μL RPMI + 1% FBS and then injected intravascularly via the retro-orbital sinus. 200 μg of CD4-depleting Ab (BioXCell, catalog no. YTS191) was injected i.p. in 100 μl of sterile PBS on days −1 and +1 postinfection (for all infections excluding TCRaKO experiments, for which no endogenous $CD4^+$ T cells were present).

Abs and flow cytometry

Single-cell suspensions of lymph nodes, spleens, livers, and lungs were stained in 50 μl of Ab mixture (10 μl of Brilliant Stain Buffer Plus, BD Biosciences, catalog no. 566385; 40 μl of MACS buffer [PBS with 0.5% BSA and 2 mM EDTA]) for 30 min at 4°C in the dark, fixed with IC Fix (Invitrogen, catalog no. 00-8222-49]) for 5 min at 4°C, and then analyzed on the BD Biosciences FACSymphony. For intracellular staining, the Foxp3 staining kit from eBiosciences (catalog no. 00-5521-11) was used per the manufacturer's instructions. Abs used for flow cytometry were used at a 1:200 dilution. The following Ab clones were used: CD8α (53-6.7, BD Biosciences), CD4 (GK1.5, BD Biosciences), CD8β (eBioH35-17.2, Invitrogen), CD45.1 (A20, BD Biosciences), CD45.2 (104, Invitrogen), live/dead fixable aqua (L34966, Invitrogen), Thy1.1 (OX-7, BioLegend), KLRG1 (2F1, Invitrogen), CX3CR1 (SA011F11, BioLegend), PD-1 (RMP1-30, BioLegend), Tim-3 (RMT3-23, BioLegend), CD69 (1H.2F3, BD Biosciences), Ly108 (13G3, BD Biosciences), granzyme A (GzA-3G8.5, Invitrogen), granzyme B (GB11, BD Biosciences), perforin (S16009A, Biolegend), CD107a (eBio1D4B, Invitrogen), IFNg (XMG1.2, BD Biosciences), TNFα (MP6-XT22, BD Biosciences), and CD62L (MEL-14, Biolegend). Analysis was performed with FlowJo (Tree Star, Ashland, OR).

In vitro peptide stimulation and CD107a mobilization assays

Single-cell suspensions of spleens and lungs were plated in 100 μl of RP-10 in round-bottomed 96-well plates; incubated with 10^{-7} M GP33 peptide (KAVYNFATM), brefeldin A (0.3 mg/μl; Sigma, catalog no. B5936), monensin (Invitrogen, ref# 00-4505-51), and 1 μl of CD107a Ab in RP-10; and then incubated for 4 h at 37°C. The cells were then stained for intracellular molecules as described above.

In vitro cytotoxicity assay

Single adoptive transfers were performed as described above, and then spleens were mashed into single-cell suspensions. $CD8^+$ T cells were isolated via negative selection by incubation with biotinylated Abs against Ter119 (Ter-119, Biolegend), CD4 (GK1.5, Invitrogen), MHCII (M5/114.15.2, eBioscience), and CD19 (eBio1D3, Invitrogen), followed by magnetic depletion with anti-streptavidin beads per the manufacturer's instructions (Miltenyi Biotec, catalog no. 130-048-101). The flow-through was collected, stained with CD45.2 APC (104, Invitrogen), and then magnetically isolated with anti-APC magnetic beads (Miltenyi Biotec, catalog no. 130-090-855) to isolate donor cells. Target cells were prepared by isolating spleens from naive mice, subjecting them to ACK lysis, and then incubating them with varying concentrations of GP33 peptide at concentrations ranging from 10^{-3} to 10^{-5} M or with no peptide at all. Peptide-loaded targets were coated with CFSE proliferation dye (eBioscience, catalog no. 5-0850-85) at 4 μM, whereas no peptide targets were coated with 0.4 μM CFSE. Then 1×10^5 target cells were cocultured with isolated effector cells for 5 h at 37°C. Ag-specific lysis was assessed via flow cytometry with the formula: 100 − [(peptide targets/no peptide targets)/(starting ratio of peptide targets/no peptide targets)] × 100.

Cell sorting and RNA isolation

Adoptive transfers were performed as described above. At 8 or 30 d postinfection (dpi), splenocytes were magnetically enriched with CD8α microbeads (Miltenyi Biotec; catalog no. 130-117-044) following the manufacturer's instructions. Adult or neonatal donor cells were sorted using the BD Biosciences FACSAria Fusion to at least 95% purity and then lysed with TRIzol (Life Technologies) to collect RNA. RNA was then isolated with chloroform extraction to remove residual phenol, and glyco-blue was added as a carrier to promote RNA precipitation. RNA concentration was determined with a Qubit and integrity assessed on a Fragment Analyzer.

RNA sequencing

Isolated RNA was used to generate libraries using the TruSeq RNA sample preparation kit (Illumina). The libraries were then sequenced using the Illumina NovaSeq6000 platform, generating 100-bp reads. Adaptors were trimmed from raw reads with trim_galore with default parameters (Babraham Bioinformatics: https://www.bioinformatics.babraham.ac.uk/projects/trim_galore/). Reads were mapped to the mm10 genome with hisat2 (20). FeatureCounts (21) was then used to count mapped reads for genomic features using GENCODE mouse gene annotation v21 (-s 0 -Q 50). Peaks with mean counts per million (CPM) across samples > = 1 were kept. The counts were transformed to log2 scale with rlog function in DESeq2 (22). Principal component analysis was performed using the prcomp function in R.

The raw counts were normalized to CPM values, and genes with CPM > 1 in at least one sample were kept for differential expression analysis. EdgeR (23, 24) was used to identify differentially expressed genes using likelihood ratio test between sample types for day 8 samples. Function gseGO in R package ClusterProfiler was used for gene set enrichment analysis for day 8 samples, with a gene list ordered by log fold changes generated from differential expression analysis as input. An additive model was fitted using sample types and pair information for day 30 samples to identify differentially expressed genes between adult and neonatal cells using edgeR. Function enrichGO in ClusterProfiler (25, 26) was used for over-representation analysis for day 30 samples, with differentially expressed genes with a false discovery rate < 0.05 as input.

LCMV quantitative real-time PCR

Blood was collected via the facial vein at 8 and 30 dpi in microcentrifuge tubes, allowed to clot for 30 min, and centrifuged at 14,000 rpm for 30 min at 4°C, and then serum was collected. Viral RNA was isolated with the Applied Biosystems 5× MagMAX-96 viral isolation kit (reference no. AMB1836-5) and the Applied Biosystems MagMAX Express 96 magnetic particle processor (catalog no. 4400074), following the manufacturer's instructions. TaqMan quantitative real-time PCR was performed using the TaqMan RNA-to-CT 1Step kit (Applied Biosystems, catalog no. 4392938), together with the following primers specific for the LCMV nucleoprotein: forward, 5′-ACTGACGAGGTCAACCCGG-3′, and reverse, 5′-CAAGTA CTCACACGGCATGGA-3′; and the probe, 5′-FAM-CTTGCCGACCTC TTCAATGCGCAA-BHQ1-3′. Measurements were collected with a Viia7 real-time PCR system (Thermo Fisher). Titered viral stocks were used as a standard curve.

Results

Neonatal CD8$^+$ T cells preferentially expand at early time points during chronic infection

The goal of this study was to examine how cell-intrinsic differences between neonatal and adult CD8$^+$ T cells alter their fates during chronic infection. Our strategy was to adoptively cotransfer an equivalent number of neonatal and adult CD8$^+$ T cells into an adult recipient and compare their number and phenotype at various times after chronic LCMV infection. By normalizing the host environment, we ensured that any observed differences between neonatal and adult cells were due to cell-intrinsic factors. We also used monoclonal CD8$^+$ T cells from P14 TCR Tg mice (specific for the LCMV gp33 protein) to control for developmentally related differences in TCR repertoire. For these experiments, small numbers (2×10^3) of CD8$^+$ T cells from neonatal (Thy1.1$^+$) and adult (Thy1.2$^+$) P14 mice were transferred into the same adult congenic recipient mice (CD45.1$^+$) (Fig. 1A, Supplemental Fig. 1A). The next day, recipient mice were systemically infected with 2×10^6 PFU LCMV clone 13 via intravascular injection, and the ratio of neonatal and adult donor CD8$^+$ T cells was determined in lymphoid (spleen) and nonlymphoid (lung) organs at different stages of infection.

Consistent with their behavior during acute infection, the neonatal CD8$^+$ T cells were the first to respond to LCMV clone 13 and outnumbered the adult cells in both the spleen and lung at 4 dpi (Fig. 1B–E, Supplemental Fig. 1B, 1C). At the peak of the response (8 dpi), the adult CD8$^+$ T cells preferentially accumulated in the spleen (Fig. 1B, 1C), whereas the neonatal cells were more abundant in the lung (Fig. 1D, 1E). However, during the chronic phase of the response (30 dpi), the numbers of neonatal and adult cells were comparable in both the spleen and the lung. Thus, the dynamics of the neonatal and adult response differed in the spleen and lung, and unlike our previous observations with acute infection, we did not observe an inability of neonatal CD8$^+$ T cells to persist in the long-lived CD8$^+$ T cell pool during chronic infection.

Given the significant numerical differences at 4 dpi, we next performed a more detailed analysis of neonatal and adult cells during early stages of infection with LCMV clone 13. First, we asked whether neonatal cells were more abundant than adult cells in other

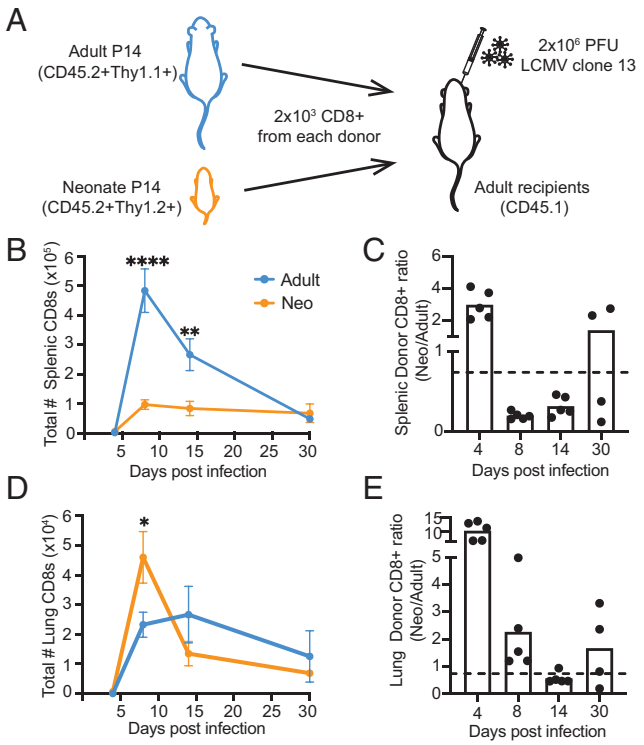

FIGURE 1. Neonatal cells preferentially expand early in chronic infection. (**A**) Schematic of experimental design. A total of 2×10^3 adult (8 to 12 wk) or neonatal (5 to 7 d) P14 CD45.2$^+$ CD8$^+$ T cells were adoptively cotransferred into wild-type adult CD45.1$^+$ recipients, which were then infected with 2×10^6 PFU LCMV clone 13 intravascularly. (**B** and **D**) Total number of CD8$^+$ T cells. (**C** and **E**) Ratio of neonatal/adult cells in the spleen and lung. The dotted line represents the starting ratio of donor cells. The data are representative of two independent experiments with $n = 4$ to 7 per time point. *$p < 0.05$, ****$p < 0.0001$, by paired two-way ANOVA with multiple comparisons.

peripheral organs shortly postinfection. Remarkably, the neonatal cells were significantly more numerous than adult cells at 4 dpi in all the organs harvested: the spleen, the inguinal lymph node, and especially the lung and liver, where there were 10-fold more neonatal than adult CD8$^+$ T cells present (Supplemental Fig. 1B–G). Notably, it was in peripheral tissues, rather than secondary lymphoid organs, where neonatal CD8$^+$ T cells had the most robust early expansion in comparison with adult CD8$^+$ T cells.

Next, we asked whether the more rapid response by neonatal cells altered their positioning in peripheral organs at 4 dpi. To address this question, we performed intravascular staining with a fluorescent Ab targeting CD8β immediately prior to euthanasia, to differentiate between cells present in the vasculature and cells that had fully migrated into tissues (27). Interestingly, only neonatal cells were present in the parenchyma of the lung and liver (Supplemental Fig. 1H, 1I), indicating that neonatal cells are indeed the first responders at sites of inflammation in the early stages of chronic infection. Thus, not only do neonatal CD8$^+$ T cells respond more quickly during chronic infection, but they also migrate out of the vasculature and into the parenchyma before adult CD8$^+$ T cells.

Neonatal CD8$^+$ T cells adopt an effector phenotype early in chronic infection

The more rapid kinetics by neonatal CD8$^+$ T cells prompted us to examine their phenotype at early stages of infection. Early in chronic infection, a KLRG1$^+$ CX3CR1$^+$ cytotoxic effector cell lineage emerges that successfully kills its targets but is short-lived

(18, 28). To determine whether neonatal or adult cells preferentially give rise to this lineage, we compared the expression of KLRG1 and CX3CR1 on both donor populations at 4 and 8 dpi using flow cytometry. At 4 dpi, nearly a quarter of splenic neonatal CD8$^+$ T cells expressed KLRG1, whereas no adult CD8$^+$ T cells expressed this marker (Fig. 2A, 2B). Importantly, neonatal CD8$^+$ T cells still expressed more KLRG1 than adult cells in both the lung and spleen at 8 dpi. Similarly, we saw expression of CX3CR1 only by neonatal cells in both the spleen and lung, but most robustly in the lung, with the majority of neonatal cells expressing CX3CR1 at 8 dpi (Fig. 2C, 2D).

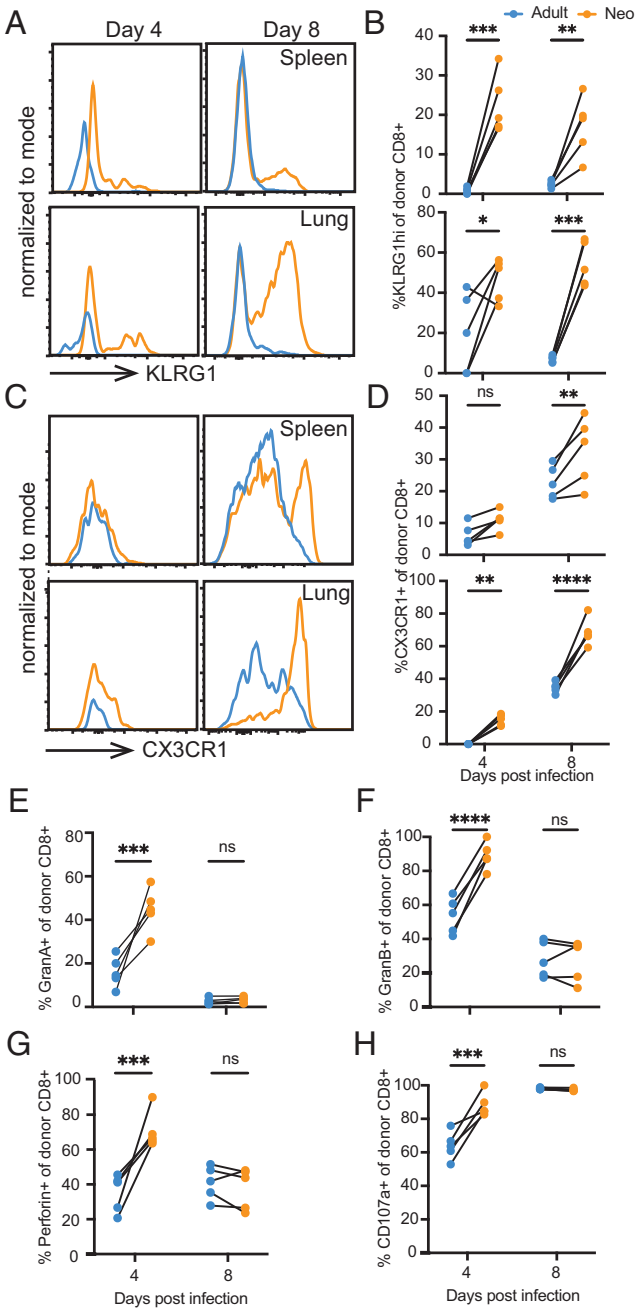

FIGURE 2. Neonatal cells adopt an effector phenotype early in chronic infection. (**A** and **C**) Representative histograms of KLRG1 (A) and CX3CR1 (C) expression on P14 adult (blue) or neonatal (orange) CD8$^+$ T cells in the spleen and lung at 4 and 8 d after LCMV clone 13 infection. (**B** and **D**) Group data of KLRG1 (B) and CX3CR1 (D) expression in the spleen and lung at 4 and 8 d postinfection (dpi). (**E**–**H**) Adult and neonatal P14 CD8$^+$ T cells were isolated at 4 and 8 dpi and restimulated with cognate peptide for 4 h. Shown are the group data of granzyme A (E), granzyme B (F), perforin (G), and CD107a (H) expression. The data are representative of two independent experiments with $n = 4$ to 7 per time point. *$p < 0.005$, ***$p < 0.001$, ****$p < 0.0001$, by paired two-way ANOVA with multiple comparisons.

It is possible that phenotypic differences by neonatal and adult CD8$^+$ T cells are due to the competitive nature of the cotransfer experiment. However, we ruled out this possibility after performing single transfer experiments and observing the same phenotypic differences in KLRG1 and CX3CR1 expression on neonatal and adult cells in a noncompetitive context (Supplemental Fig. 2A–C). We also considered that neonatal and adult CD8$^+$ T cells may express different amounts of these markers even prior to infection. To examine this possibility, we performed phenotypic analysis of adult and neonatal P14 CD8$^+$ T cells before adoptive transfer, and we found that they both exhibited a naive phenotype and expressed similarly low levels of markers typically observed in effector and memory cells (Supplemental Fig. 2D). We also examined other phenotypic markers that have more recently been used to identify the exhausted precursors (TCF-1/Ly108$^+$, Tim3$^-$) and effector-like cells (TCF-1/Ly108$^-$, Tim3$^+$) soon after chronic infection (29, 30). The neonatal CD8$^+$ T cells expressed less Ly108 and more Tim3 in the spleen and the lung at 4 and 8 dpi (Supplemental Fig. 2E–J), which is consistent with the neonatal bias toward an effector fate early after chronic infection. Collectively, these data demonstrate that phenotypic differences between neonatal and adult CD8$^+$ T cells are not due to changes present in the starting population or the competitive nature of the experimental approach, but rather due to an inherent propensity of neonatal cells to adopt an effector phenotype during the early stages of chronic infection.

Adoption of an effector-like phenotype does not specifically address functionality, so we next asked whether the production of effector molecules was different in neonatal and adult CD8$^+$ T cells during early chronic infection. On days 4 and 8 postinfection, we performed a peptide restimulation assay to measure production of effector molecules. Neonatal CD8$^+$ T cells produced more granzyme A, granzyme B, and perforin at 4 dpi, but not at 8 dpi (Fig. 2E–G, Supplemental Fig. 2K). We also performed a CD107a mobilization assay and found significantly more CD107a expression by neonatal CD8$^+$ T cells at 4 dpi, but not at 8 dpi (Fig. 2H, Supplemental Fig. 2K). Thus, not only do neonatal CD8$^+$ T cells produce more cytotoxic molecules, but they also have a greater ability to degranulate very early in chronic infection. Because peptide restimulation assays do not assess the full process of cytotoxicity, we performed an in vitro cytotoxicity assay with donor cells isolated on D8 from the spleen. The neonatal CD8$^+$ T cells killed significantly more target cells than adult cells (Supplemental Fig. 2L), indicating that their cytotoxic potential outperforms their adult counterparts even at 8 dpi. The fact that effector functions were more robust in neonatal cells at early time points suggests they are the first to offer protective functions during chronic infection.

Neonatal and adult CD8$^+$ T cells exhibit distinct gene expression profiles at the peak of the response

Our data up to this point suggest that neonatal CD8$^+$ T cells preferentially adopt an effector phenotype during early stages of chronic infection. However, our conclusion is largely based on the expression of a small number of surface receptors (KLRG1, CX3CR1, Ly108, and Tim3) and limited functional assays. To take an unbiased approach at characterizing the neonatal and adult early responses to chronic infection, we performed RNA sequencing. After adoptive transfer of CD8$^+$ T cells from neonatal and adult P14 mice into wild-type recipients and infection of recipient mice with LCMV clone 13 (Fig. 3A), donor cells in the spleen were

sorted at 8 dpi and subjected to RNA sequencing. Adult and neonatal CD8$^+$ T cells showed global transcriptomic differences upon principal component analysis, with age-related clustering driving PC1, which accounted for 40.03% of the observed variance between groups (Fig. 3B). We observed 196 differently expressed genes between the two populations. Upon performing gene set enrichment analysis on Gene Ontology biological processes, the neonatal samples showed more activated immune responses and a stronger defense response to other organisms (Fig. 3C), supporting our previous findings that neonatal cells display an early effector phenotype and superior cytotoxic functions. Gene set enrichment analysis also revealed that neonatal CD8$^+$ T cells had more robust migratory capabilities and distinct cell adhesion and migration patterns, consistent with their early migration to the lung and extravasation into parenchymal tissue.

Further delving into individual genes related to pathways of interest, we found the lymphoid-homing receptor, *Sell* (CD62L), to be less expressed in neonatal CD8$^+$ T cells, whereas the lung-homing receptor, CCR5, was more expressed, consistent with their early propensity to migrate away from the spleen (Fig. 3D). Neonatal cells also expressed more effector genes like *GzmA* (granzyme A), *GzmB* (granzyme B), *GzmK* (granzyme K), *Prf1* (perforin), *Ifng* (IFNγ), and *KLRG1*, suggesting that their effector phenotype and function extends beyond the limited markers we previously selected for flow cytometry. Importantly, adult CD8$^+$ T cells expressed more antiapoptotic molecules like *Bcl2* and fewer proapoptotic molecules like *FasL*, suggesting that the bias away from the effector lineage by adult cells comes at the benefit of greater cell viability, consistent with the fact that they outnumber neonatal CD8$^+$ T cells in the spleen at 8 dpi.

Neonatal CD8$^+$ T cells are less exhausted at chronic time points

After establishing how cell-intrinsic differences between neonatal and adult CD8$^+$ T cells alter cell fate decisions during early stages of infection, we next shifted our focus to the chronic phase of infection (30 dpi), when the exhaustion program is stable (19). A key question is whether the neonatal or adult cells are more exhausted during this phase of infection. Coexpression of PD-1 and Tim3 can be used to identify the most exhausted subpopulation of CD8$^+$ T cells responding to a chronic Ag (31–34). Thus, we examined expression of PD-1 and Tim3 in cotransferred neonatal and adult P14 cells at 30 dpi. We found a significantly higher percentage of PD1$^+$Tim3$^+$ cells in the adult CD8$^+$ T cell pool compared with the neonatal pool in both the spleen and the lung (Fig. 4A, 4B). We also analyzed the individual geometric mean fluorescence intensity of PD-1 and Tim3, which indicated that the smaller exhausted neonatal pool was driven specifically by less Tim-3 expression in the spleen, whereas neonatal cells expressed lower amounts of both Tim3 and PD-1 in the lung (Supplemental Fig. 3A, 3B). We next wondered whether neonatal cells in the lung on day 30 still retained expression of KLRG1. Indeed, ~45% of the neonatal cells in the lung expressed KLRG1, compared with only 5% of adult cells (Fig. 4C). Neonatal cells in the lung also expressed significantly more CX3CR1 than their adult counterparts at 30 dpi (Supplemental Fig. 3C). To determine whether their altered phenotype was associated with differences in their microanatomical location, we performed

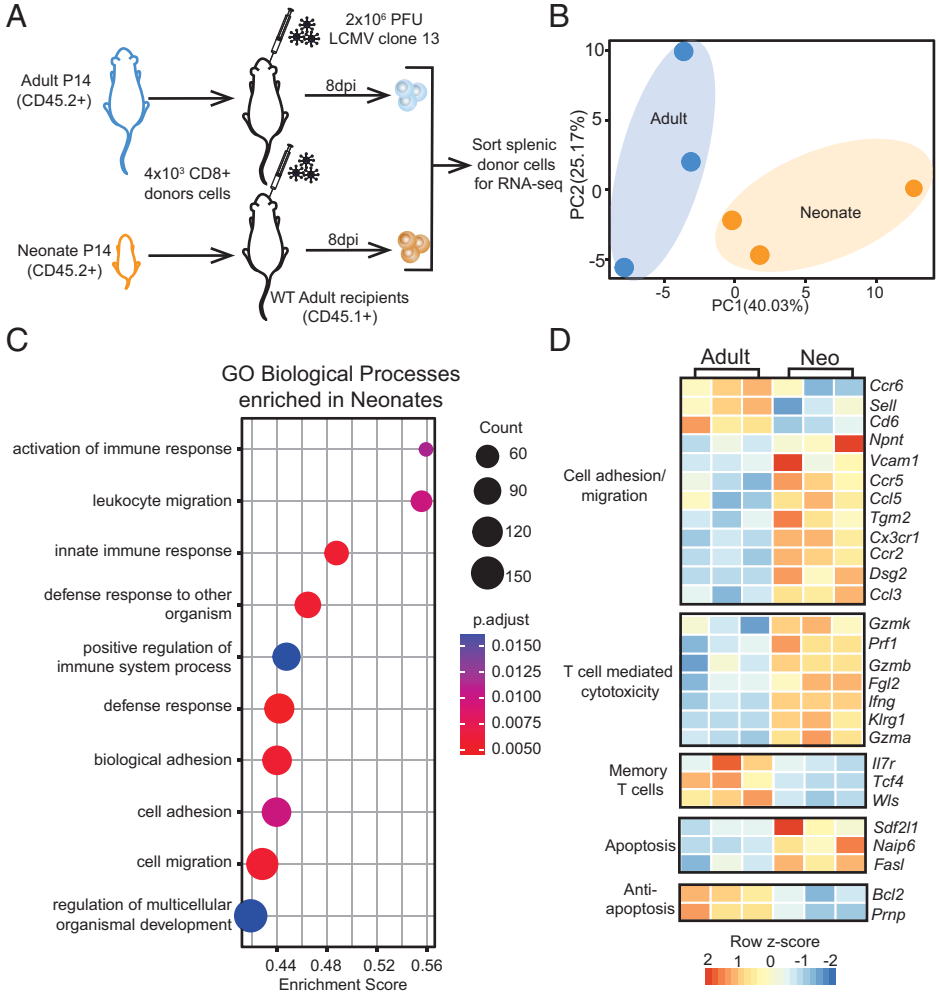

FIGURE 3. Neonatal cells are transcriptionally distinct at 8 d postinfection (dpi). (**A**) Schematic of experimental design. A total of 4 × 10^3 adult or neonatal P14 CD8$^+$ T cells (CD45.2$^+$) were adoptively transferred into wild-type (WT) adult recipients (CD45.1$^+$), which were then infected with 2 × 10^6 PFU LCMV clone 13. Splenic donor cells were sorted to 95% purity at 8 dpi and then subjected to RNA sequencing (RNA-seq). (**B**) Principal component analysis plot representing global transcriptomic differences between neonatal (orange) and adult (blue) cells. (**C**) Gene sets more highly expressed in neonatal cells, as identified by GO enrichment analysis. (**D**) Heat map of individual genes related to cell adhesion and migration, T cell–mediated cytotoxicity, memory T cells, apoptosis, and antiapoptosis. GO, Gene Ontology.

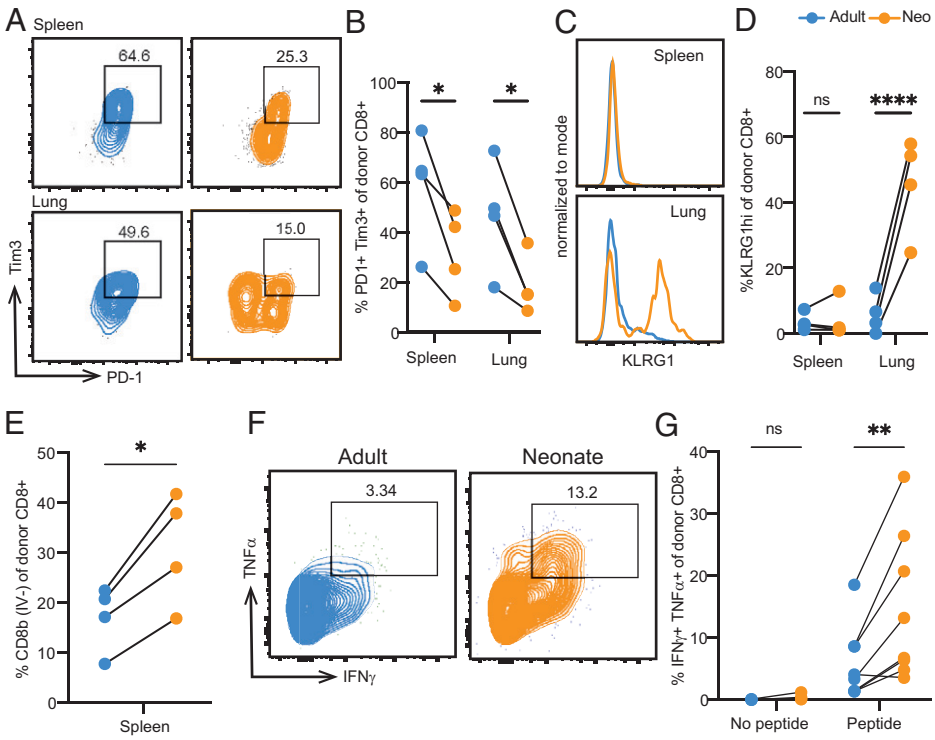

FIGURE 4. Neonatal cells are less exhausted at 30 postinfection (dpi). Adoptive cotransfer was performed as described for Fig. 1A. (**A** and **B**) Representative contour plots (A) and group data (B) of PD-1$^+$ Tim3$^+$ adult and neonatal P14 CD8$^+$ T cells in the spleen and lung at 30 dpi. (**C**) Representative histogram and (**D**) group data of KLRG1 expression at 30 dpi in the spleen and lung. (**E**) Percentage of intravascular-negative donor cells in the spleen at 30 dpi. (**F** and **G**) Adult and neonatal P14 CD8$^+$ T cells were isolated from the spleen at 30 dpi and restimulated with cognate peptide for 4 h. Representative contour plots (F) and group data (G) of TNF and IFN-γ production are shown. The data are representative of two independent experiments with $n = 4$ to 7 per time point. (A–D, F, and G) $*p < 0.05$, $**p < 0.01$, $***p < 0.001$, $****p < 0.0001$, by paired two-way ANOVA with multiple comparisons. (E) $*p < 0.05$, by paired two-tailed Student *t* test.

intravascular staining of adult and neonatal CD8$^+$ T cells at 30 dpi and found significantly more neonatal cells in the vasculature-negative population in the spleen (Fig. 4E). These data suggest that the bias toward more differentiated effectors and distinct homing properties early postinfection may result in fewer neonatal cells becoming exhausted during the later stages of infection.

To gain deeper insight into the phenotypic differences between neonatal and adult cells at 30 dpi, we also further subsetted the donor cells into exhausted progenitors (Ly108$^+$ CX3CR1$^-$), terminally exhausted cells (Ly108$^-$, CX3CR1$^-$), and effector cells (Ly108$^-$, CX3CR1$^+$) (35, 36). Indeed, neonatal CD8$^+$ T cells expressed more Ly108 and more CX3CR1 when compared with their adult counterparts in both the spleen and the lung (Supplemental Fig. 3D–G), revealing a heterogeneous 30 dpi neonatal pool that skews away from a terminally exhausted phenotype and toward an effector-like phenotype (Ly108$^-$ CX3CR1$^+$) or an exhausted-progenitor phenotype (Ly108$^+$ CX3CR1$^-$). However, the majority of adult cells in the spleen and the lung adopted a terminally exhausted phenotype (Ly108$^-$ CX3CR1$^-$). The Ly108$^-$ CX3CR1$^+$ effector cells can be further subdivided according to their expression of KLRG1 (30, 37). Within the Ly108$^-$ CX3CR1$^+$ effector subset, nearly 80% of neonatal CD8$^+$ T cells, but less than 20% of adult cells, expressed KLRG1 (Supplemental Fig. 3F). Clearly, neonatal CD8$^+$ T cells have a cell-intrinsic propensity for adopting an effector phenotype and resisting terminal exhaustion at the chronic time point.

Exhausted phenotypes must also be validated with functional assays. We know that chronic TCR stimulation leads to the hierarchical loss of TNFα production, followed by the loss of IFNγ production (11), which is a main reason why exhausted CD8$^+$ T cells are unsuccessful at clearing chronic infections and tumors. Thus, we isolated adult and neonatal P14 CD8$^+$ T cells at 30 dpi and incubated them with their cognate peptide for 4 h in the presence of brefeldin A. We found significantly more polyfunctional IFNγ$^+$ TNFα$^+$ cells in the neonatal pool than the adult pool (Fig. 4F, 4G) but slightly fewer granzyme A-producing cells (Supplemental Fig. 3G). The higher number of neonatal cells producing both IFNγ and TNFα but fewer cytotoxic molecules is consistent with our finding that neonatal cells are less exhausted than their adult counterparts.

Neonatal CD8$^+$ T cells exhibit a more effector-like gene expression profile during the chronic phase of infection

To take an unbiased approach to characterizing the neonatal CD8$^+$ T cell response in the chronic phase of infection, we isolated RNA from adult and neonatal P14 CD8$^+$ T cells that had been cotransferred into recipient mice and then infected for 30 d with LCMV cl13 (Fig. 5A). We found that neonatal CD8$^+$ T cells had 489 differentially expressed genes when compared with their adult counterparts. When Gene Ontology analysis was performed on biological processes, T cell activation, immune effector processes, adaptive immune response, leukocyte migration, and mononuclear cell migration were the top five pathways upregulated in neonatal samples (Fig. 5B). Our global characterization validated that the neonatal population is indeed more activated and migratory than their adult counterparts at the chronic phase of infection.

Next, we took a more granular approach and examined key differentially expressed genes between the two populations. Three categories of genes can summarize the differences: genes related to phenotype, signaling, and migration (Fig. 5C). First, under the phenotype category, neonatal cells expressed more *KLRG1* and *CX3CR1*, indicating that neonatal cells retain an effector phenotype in the spleen at the chronic phase of infection. Neonatal cells also expressed several NK cell markers, like *KLRK1*, *KLRE1*, and *KLRb1c*, whose expression was recently linked to sustained cytotoxicity during chronic infection (37). However, adult cells expressed more transcripts related to exhaustion, such as *CD244a*, *CD200r1*, *Entpd1*, *CTLA4*, and *Pdcd1*, suggesting divergent fates at the chronic time point.

Second, we observed notable differences in the expression of signaling molecules in neonatal and adult cells. In general, the neonatal cells expressed higher levels of genes that promote effector cell differentiation (*Zeb2*, *Tbx21*) (38, 39) and are typically downregulated

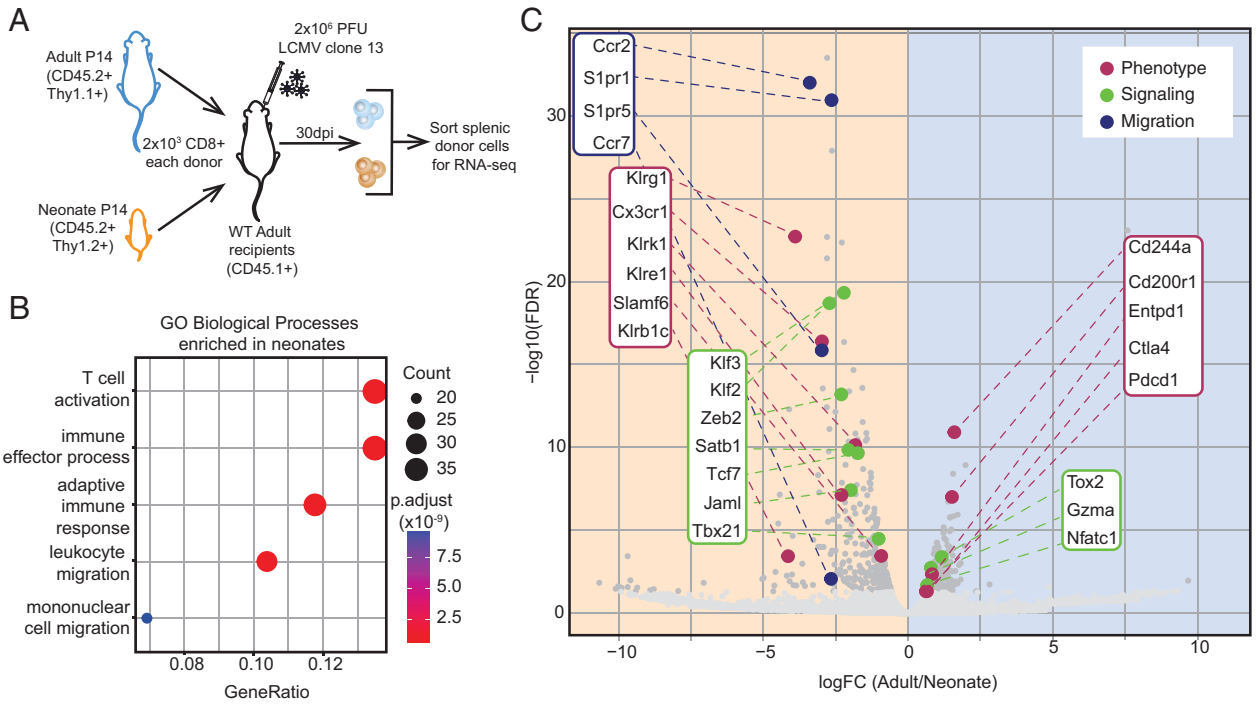

FIGURE 5. Neonatal cells are transcriptionally distinct at the chronic phase of infection. (**A**) Schematic of experimental design. A total of 2×10^3 adult (8 to 12 wk) or neonatal (5 to 7 d) P14 CD45.2$^+$ CD8$^+$ T cells were adoptively cotransferred into wild-type (WT) adult CD45.1$^+$ recipients, which were then infected with 2×10^6 PFU LCMV clone 13 intravascularly. Splenic donor cells were sorted to 95% purity at 30 dpi and then subjected to RNA sequencing (RNA-seq). (**B**) Gene sets over-represented in genes more highly expressed in neonatal cells. (**C**) Volcano plot of differentially expressed genes upregulated in neonatal cells (orange background) or adult cells (blue background). Genes of interest related to phenotype are indicated in red, signaling is in green, and migration is in blue. FDR, false discovery rate; GO, Gene Ontology.

in exhausted cells (*Klf2*, *Klf3*, *Satb1*) (40, 41). However, a gene known to maintain stem-like exhausted progenitors (*Tcf7*) was also elevated in neonatal cells (18), suggesting that there may be additional heterogeneity in the neonatal pool at the chronic time point. In contrast, the signaling molecules upregulated in adult cells included *Nfatc* and *Tox2*, which are necessary for reprogramming CD8$^+$ T cells into the exhausted differentiation trajectory (42, 43). Together, these results indicate that neonatal CD8$^+$ T cells express fewer signaling molecules related to exhaustion than adult cells at 30 dpi.

Finally, genes related to migration were only identified in neonatal cells and not in adult cells. Neonatal cells expressed receptors that cause migration to peripheral tissues and lymphoid egress, such as *CCR2*, *S1pr5*, and *S1pr1* (44–46). However, they also expressed more *CCR7*, which is critical to migration to and through lymphoid organs (47). The migratory neonatal signature specific to both lymphoid location and peripheral tissue localization is likely explained by subset variability between neonatal and adult cells. Collectively, our data show striking transcriptional differences between adult and neonatal CD8$^+$ T cells responding to chronic infection.

Neonatal cells protect against viral replication during chronic infection

Considering the robust differences between adult and neonatal CD8$^+$ T cell phenotype and function at both early and late time points in chronic infection, we next tested whether these observed differences altered disease outcome. To create an environment where adult or neonatal P14 CD8$^+$ T cells responded to chronic infection in isolation, without the influence of other CD8$^+$ T cells on viral progression, we adoptively transferred adult or neonatal P14 CD8$^+$ T cells into separate recipient mice lacking a T cell compartment (TCR$\alpha^{-/-}$ mice); then, we infected all recipients the next day with LCMV clone 13 (Fig. 6A).

The mice that received neonatal donor CD8$^+$ T cells prior to LCMV clone 13 infection lost significantly less weight and recovered from their weight loss more quickly compared with recipients that received adult cells (Fig. 6B). To determine whether differences in weight loss corresponded to changes in viral replication, we collected serum from both groups of recipient mice at 8 and 30 dpi and performed quantitative real-time PCR with primers specific to LCMV clone 13. Sera from mice that received neonatal cells had significantly fewer viral copies at 8 dpi but not at 30 dpi, suggesting that neonatal CD8$^+$ T cells offer greater protection from viral replication early in chronic infection (Fig. 6C). Together, our data show that the cell-intrinsic differences between adult and neonatal CD8$^+$ T cells responding to chronic infection impart a functional bias that corresponds to different disease outcomes.

Discussion

Previous work has demonstrated that cell-intrinsic differences between neonatal and adult T cells alter their differentiation trajectories after acute infection and vaccination (4, 6, 7). In this article, we extend this work by showing that neonatal CD8$^+$ T cells have a distinct response to chronic infection from adult CD8$^+$ T cells. Using a coadoptive transfer approach, we found that neonatal CD8$^+$ T cells preferentially give rise to effector cells that express KLRG1 and CX3CR1, even when exposed to the same amount of Ag and inflammation as their adult counterparts. Neonatal CD8$^+$ T cells were significantly less exhausted at chronic time points, and they curbed viral replication at earlier time points in infection. Altogether, our work shows that cell-intrinsic differences between neonatal and adult CD8$^+$ T cells

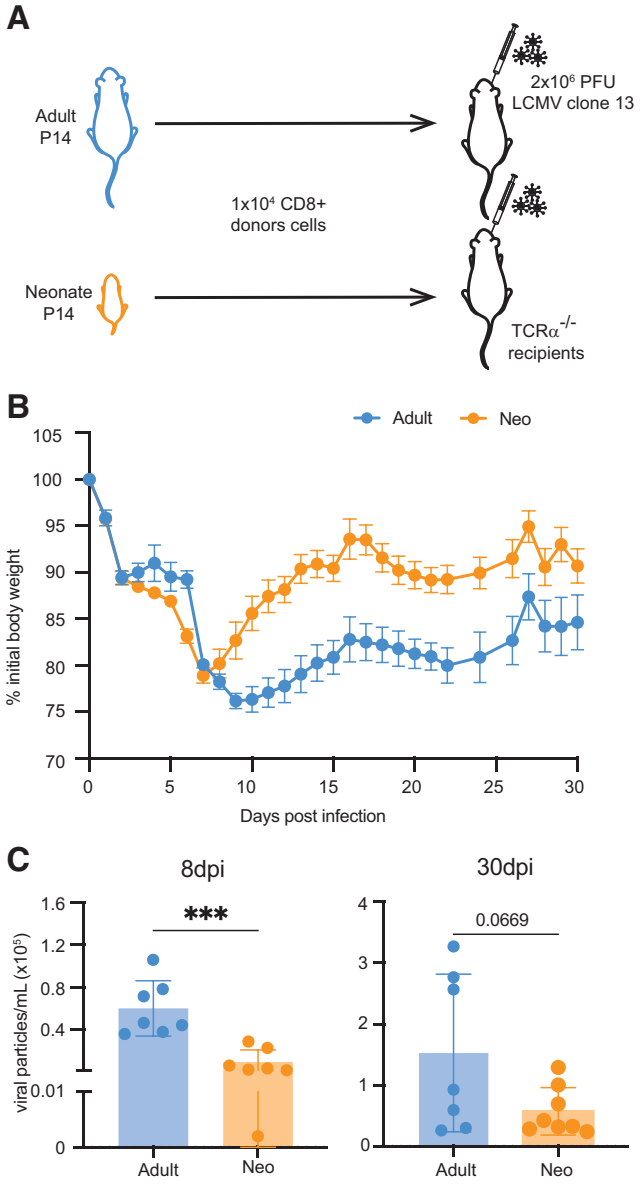

FIGURE 6. Neonatal cells protect against viral replication. (**A**) Schematic of experimental design. A total of 1×10^4 adult or neonatal P14 $CD8^+$ T cells were transferred into $TCR\alpha^{-/-}$ recipient mice, which were infected 1 day later with 2×10^6 PFU LCMV clone 13. (**B**) Percentage of initial body weight postinfection. (**C**) Viral copies per mL serum at 8 and 30 d postinfection (dpi), measured by quantitative real-time PCR with fluorescent probe against the LCMV nucleoprotein. The data are representative of two independent experiments with $n = 4$ to 8 per time point. $^*p < 0.05$, $^{***}p < 0.001$, by two-tailed Student t test.

affect cell fate decisions and clinical manifestations of disease during chronic infection.

One of the most interesting findings in our study is that neonatal cells are inherently more resistant to exhaustion during chronic infection than adult cells. There are several reasons why this might be the case. First, the enhanced ability of neonatal $CD8^+$ T cells to extravasate and migrate into peripheral tissues very early during infection may protect them from prolonged Ag exposure throughout chronic infection. Second, the more effector-like chromatin state of neonatal cells prior to infection (5) may limit their ability to differentiate into certain types of long-lived cells, including exhausted cells. Third, all of the neonatal $CD8^+$ T cells are recent thymic emigrants, whereas the adult $CD8^+$ T cells have undergone more postthymic maturation, which may affect their differentiation trajectories during chronic infection (48, 49). Experiments to understand the relative contribution of these possibilities would provide key insights into why $CD8^+$ T cells made at different stages of life undergo different degrees of exhaustion during chronic infection.

The fact that adult cells are more prone to clonal exhaustion has important implications for how we approach adoptive immunotherapies. For example, a promising therapeutic strategy for treating cancer involves the use of chimeric Ag receptor (CAR) T cells: T cells are isolated from the peripheral blood, re-engineered to express a CAR, and injected back into the patient so they can mount an immune response against cancer cells (50–52). However, most CAR T cells are made with adult T cells, and although they have the potential to lead to complete regression of advanced cancer in some patients, the overall response rates are still variable, and the upregulation of T cell exhaustion markers (e.g., PD-1 and Tim3) are still a critical barrier to success (53). Our findings raise the possibility that CAR T cells could be made more resistant to exhaustion (and thereby more effective) by using neonatal T cells. Support for this idea can be found in other studies demonstrating that T cells from umbilical cord blood express lower amounts of inhibitory receptors than those from adult peripheral blood and generally mount a more robust antitumor response (54).

It is also important to consider that neonatal cells' inherent ability to resist exhaustion may actually be harmful to the host in early life. Clonal exhaustion has been shown to be an important mechanism protecting the host against excessive immunopathology during chronic infection (55, 56). Exhausted $CD8^+$ T cells are not completely inert and still exert immune pressure during chronic infection (8, 57). Therefore, clonal exhaustion can also be viewed as a useful adaptation by which $CD8^+$ T cells are able to limit tissue damage while still providing a level of immune control. Based on the findings in our study, we may speculate that chronic infection causes more overt symptoms of disease in neonates and infants not because $CD8^+$ T cells respond poorly or cannot control the viral replication but rather because their $CD8^+$ T cells are less able to establish a host–pathogen stalemate and instead cause more immunopathology.

Lastly, future work will be important for understanding how environmental factors contribute to age-related differences in the $CD8^+$ T cell response to chronic infection. It will also be important to determine how long the altered fates of neonatal and adult $CD8^+$ T cells persist postinfection and link the behavior of $CD8^+$ T cells during adult chronic infections with their developmental origins. We previously found that neonatal $CD8^+$ T cells persist into adulthood and retain their cell-intrinsic properties during acute infection (5). However, it remains unclear whether the spectrum of exhausted states observed during chronic infection relates to the age at which the responding cells were made. The studies in this report represent an important first step toward understanding how $CD8^+$ T cell ontogeny affects the host response to chronic infections.

Disclosures

E.J.W. is an advisor for Danger Bio, Marengo, Janssen, NewLimit, Pluto Immunotherapeutics Related Science, Santa Ana Bio, Synthekine, and Surface Oncology. E.J.W. is a founder of and holds stock in Surface Oncology, Danger Bio, and Arsenal Biosciences. The other authors have no conflicts of interest.

References

1. Borghesi, A., A. Marzollo, A. Michev, and J. Fellay. 2020. Susceptibility to infection in early life: a growing role for human genetics. *Hum. Genet.* 139: 733–743.

2. Chuang, Y. Y., and Y. C. Huang. 2019. Enteroviral infection in neonates. *J. Microbiol. Immunol. Infect.* 52: 851–857.
3. Strunk, T., S. E. Jamieson, and D. Burgner. 2013. Genetic and epigenetic susceptibility to early life infection. *Curr. Opin. Infect. Dis.* 26: 241–247.
4. Tabilas, C., J. Wang, X. Liu, J. W. Locasale, N. L. Smith, and B. D. Rudd. 2019. Cutting edge: elevated glycolytic metabolism limits the formation of memory CD8$^+$ T cells in early life. *J. Immunol.* 203: 2571–2576.
5. Smith, N. L., R. K. Patel, A. Reynaldi, J. K. Grenier, J. Wang, N. B. Watson, K. Nzingha, K. J. Yee Mon, S. A. Peng, A. Grimson, et al. 2018. Developmental origin governs CD8$^+$ T cell fate decisions during infection. *Cell* 174: 117–130.e14.
6. Wang, J., E. M. Wissink, N. B. Watson, N. L. Smith, A. Grimson, and B. D. Rudd. 2016. Fetal and adult progenitors give rise to unique populations of CD8$^+$ T cells. *Blood* 128: 3073–3082.
7. Smith, N. L., E. Wissink, J. Wang, J. F. Pinello, M. P. Davenport, A. Grimson, and B. D. Rudd. 2014. Rapid proliferation and differentiation impairs the development of memory CD8$^+$ T cells in early life. *J. Immunol.* 193: 177–184.
8. McLane, L. M., M. S. Abdel-Hakeem, and E. J. Wherry. 2019. CD8 T cell exhaustion during chronic viral infection and cancer. *Annu. Rev. Immunol.* 37: 457–495.
9. Moskophidis, D., F. Lechner, H. Pircher, and R. M. Zinkernagel. 1993. Virus persistence in acutely infected immunocompetent mice by exhaustion of antiviral cytotoxic effector T cells. [Published erratum appears in 1993 *Nature* 364: 262.] *Nature* 362: 758–761.
10. Ahmed, R., A. Salmi, L. D. Butler, J. M. Chiller, and M. B. Oldstone. 1984. Selection of genetic variants of lymphocytic choriomeningitis virus in spleens of persistently infected mice. Role in suppression of cytotoxic T lymphocyte response and viral persistence. *J. Exp. Med.* 160: 521–540.
11. Wherry, E. J., J. N. Blattman, K. Murali-Krishna, R. van der Most, and R. Ahmed. 2003. Viral persistence alters CD8 T-cell immunodominance and tissue distribution and results in distinct stages of functional impairment. *J. Virol.* 77: 4911–4927.
12. Wherry, E. J., and M. Kurachi. 2015. Molecular and cellular insights into T cell exhaustion. *Nat. Rev. Immunol.* 15: 486–499.
13. Frebel, H., V. Nindl, R. A. Schuepbach, T. Braunschweiler, K. Richter, J. Vogel, C. A. Wagner, D. Loffing-Cueni, M. Kurrer, B. Ludewig, and A. Oxenius. 2012. Programmed death 1 protects from fatal circulatory failure during systemic virus infection of mice. *J. Exp. Med.* 209: 2485–2499.
14. Mueller, S. N., V. K. Vanguri, S. J. Ha, E. E. West, M. E. Keir, J. N. Glickman, A. H. Sharpe, and R. Ahmed. 2010. PD-L1 has distinct functions in hematopoietic and nonhematopoietic cells in regulating T cell responses during chronic infection in mice. *J. Clin. Invest.* 120: 2508–2515.
15. Sun, C., R. Mezzadra, and T. N. Schumacher. 2018. Regulation and function of the PD-L1 checkpoint. *Immunity* 48: 434–452.
16. Im, S. J., M. Hashimoto, M. Y. Gerner, J. Lee, H. T. Kissick, M. C. Burger, Q. Shan, J. S. Hale, J. Lee, T. H. Nasti, et al. 2016. Defining CD8$^+$ T cells that provide the proliferative burst after PD-1 therapy. *Nature* 537: 417–421.
17. Barber, D. L., E. J. Wherry, D. Masopust, B. Zhu, J. P. Allison, A. H. Sharpe, G. J. Freeman, and R. Ahmed. 2006. Restoring function in exhausted CD8 T cells during chronic viral infection. *Nature* 439: 682–687.
18. Chen, Z., Z. Ji, S. F. Ngiow, S. Manne, Z. Cai, A. C. Huang, J. Johnson, R. P. Staupe, B. Bengsch, C. Xu, et al. 2019. TCF-1–centered transcriptional network drives an effector versus exhausted CD8 T cell-fate decision. *Immunity* 51: 840–855.e5.
19. Angelosanto, J. M., S. D. Blackburn, A. Crawford, and E. J. Wherry. 2012. Progressive loss of memory T cell potential and commitment to exhaustion during chronic viral infection. *J. Virol.* 86: 8161–8170.
20. Kim, D., J. M. Paggi, C. Park, C. Bennett, and S. L. Salzberg. 2019. Graph-based genome alignment and genotyping with HISAT2 and HISAT-genotype. *Nat. Biotechnol.* 37: 907–915.
21. Liao, Y., G. K. Smyth, and W. Shi. 2014. featureCounts: an efficient general purpose program for assigning sequence reads to genomic features. *Bioinformatics* 30: 923–930.
22. Love, M. I., W. Huber, and S. Anders. 2014. Moderated estimation of fold change and dispersion for RNA-seq data with DESeq2. *Genome Biol.* 15: 550.
23. McCarthy, D. J., Y. Chen, and G. K. Smyth. 2012. Differential expression analysis of multifactor RNA-Seq experiments with respect to biological variation. *Nucleic Acids Res.* 40: 4288–4297.
24. Robinson, M. D., D. J. McCarthy, and G. K. Smyth. 2010. edgeR: a Bioconductor package for differential expression analysis of digital gene expression data. *Bioinformatics* 26: 139–140.
25. Wu, T., E. Hu, S. Xu, M. Chen, P. Guo, Z. Dai, T. Feng, L. Zhou, W. Tang, L. Zhan, et al. 2021. clusterProfiler 4.0: a universal enrichment tool for interpreting omics data. *Innovation (Camb.)* 2: 100141.
26. Yu, G., L. G. Wang, Y. Han, and Q. Y. He. 2012. clusterProfiler: an R package for comparing biological themes among gene clusters. *OMICS* 16: 284–287.
27. Anderson, K. G., H. Sung, C. N. Skon, L. Lefrancois, A. Deisinger, V. Vezys, and D. Masopust. 2012. Cutting edge: intravascular staining redefines lung CD8 T cell responses. *J. Immunol.* 189: 2702–2706.
28. Chen, Y., R. A. Zander, X. Wu, D. M. Schauder, M. Y. Kasmani, J. Shen, S. Zheng, R. Burns, E. J. Taparowsky, and W. Cui. 2021. BATF regulates progenitor to cytolytic effector CD8$^+$ T cell transition during chronic viral infection. *Nat. Immunol.* 22: 996–1007.
29. Marx, A. F., S. M. Kallert, T. M. Brunner, J. A. Villegas, F. Geier, J. Fixemer, T. Abreu-Mota, P. Reuther, W. V. Bonilla, J. Fadejeva, et al. 2023. The alarmin interleukin-33 promotes the expansion and preserves the stemness of Tcf-1$^+$ CD8$^+$ T cells in chronic viral infection. *Immunity* 56: 813–828.e10.
30. Giles, J. R., S. F. Ngiow, S. Manne, A. E. Baxter, O. Khan, P. Wang, R. Staupe, M. S. Abdel-Hakeem, H. Huang, D. Mathew, et al. 2022. Shared and distinct biological circuits in effector, memory and exhausted CD8$^+$ T cells revealed by temporal single-cell transcriptomics and epigenetics. *Nat. Immunol.* 23: 1600–1613.
31. Anderson, A. C., N. Joller, and V. K. Kuchroo. 2016. Lag-3, Tim-3, and TIGIT: co-inhibitory receptors with specialized functions in immune regulation. *Immunity* 44: 989–1004.
32. Gorman, J. V., and J. D. Colgan. 2014. Regulation of T cell responses by the receptor molecule Tim-3. *Immunol. Res.* 59: 56–65.
33. Sakuishi, K., P. Jayaraman, S. M. Behar, A. C. Anderson, and V. K. Kuchroo. 2011. Emerging Tim-3 functions in antimicrobial and tumor immunity. *Trends Immunol.* 32: 345–349.
34. Golden-Mason, L., B. E. Palmer, N. Kassam, L. Townshend-Bulson, S. Livingston, B. J. McMahon, N. Castelblanco, V. Kuchroo, D. R. Gretch, and H. R. Rosen. 2009. Negative immune regulator Tim-3 is overexpressed on T cells in hepatitis C virus infection and its blockade rescues dysfunctional CD4$^+$ and CD8$^+$ T cells. *J. Virol.* 83: 9122–9130.
35. Baxter, A. E., H. Huang, J. R. Giles, Z. Chen, J. E. Wu, S. Drury, K. Dalton, S. L. Park, L. Torres, B. W. Simone, et al. 2023. The SWI/SNF chromatin remodeling complexes BAF and PBAF differentially regulate epigenetic transitions in exhausted CD8$^+$ T cells. *Immunity* 56: 1320–1340.e10.
36. Zander, R., D. Schauder, G. Xin, C. Nguyen, X. Wu, A. Zajac, and W. Cui. 2019. CD4$^+$ T cell help is required for the formation of a cytolytic CD8$^+$ T cell subset that protects against chronic infection and cancer. *Immunity* 51: 1028–1042.e4.
37. Daniel, B., K. E. Yost, S. Hsiung, K. Sandor, Y. Xia, Y. Qi, K. J. Hiam-Galvez, M. Black, C. J Raposo, Q. Shi, et al. 2022. Divergent clonal differentiation trajectories of T cell exhaustion. *Nat. Immunol.* 23: 1614–1627.
38. Kasmani, M. Y., R. Zander, H. K. Chung, Y. Chen, A. Khatun, M. Damo, P. Topchyan, K. E. Johnson, D. Levashova, R. Burns, et al. 2023. Clonal lineage tracing reveals mechanisms skewing CD8$^+$ T cell fate decisions in chronic infection. *J. Exp. Med.* 220: e20220679.
39. Kao, C., K. J. Oestreich, M. A. Paley, A. Crawford, J. M. Angelosanto, M. A. Ali, A. M. Intlekofer, J. M. Boss, S. L. Reiner, A. S. Weinmann, and E. J. Wherry. 2011. Transcription factor T-bet represses expression of the inhibitory receptor PD-1 and sustains virus-specific CD8$^+$ T cell responses during chronic infection. *Nat. Immunol.* 12: 663–671.
40. Wherry, E. J., S. J. Ha, S. M. Kaech, W. N. Haining, S. Sarkar, V. Kalia, S. Subramaniam, J. N. Blattman, D. L. Barber, and R. Ahmed. 2007. Molecular signature of CD8$^+$ T cell exhaustion during chronic viral infection. [Published erratum appears in 2007 *Immunity* 27: 824.] *Immunity* 27: 670–684.
41. Stephen, T. L., K. K. Payne, R. A. Chaurio, M. J. Allegrezza, H. Zhu, J. Perez-Sanz, A. Perales-Puchalt, J. M. Nguyen, A. E. Vara-Ailor, E. B. Eruslanov, et al. 2017. SATB1 expression governs epigenetic repression of PD-1 in tumor-reactive T cells. *Immunity* 46: 51–64.
42. Khan, O., J. R. Giles, S. McDonald, S. Manne, S. F. Ngiow, K. P. Patel, M. T. Werner, A. C. Huang, K. A. Alexander, J. E. Wu, et al. 2019. TOX transcriptionally and epigenetically programs CD8$^+$ T cell exhaustion. *Nature* 571: 211–218.
43. Seo, H., J. Chen, E. González-Avalos, D. Samaniego-Castruita, A. Das, Y. H. Wang, I. F. López-Moyado, R. O. Georges, W. Zhang, A. Onodera, et al. 2019. TOX and TOX2 transcription factors cooperate with NR4A transcription factors to impose CD8$^+$ T cell exhaustion. [Published erratum appears in 2019 *Proc. Natl. Acad. Sci. U.S.A.* 16: 19761.] *Proc. Natl. Acad. Sci. U.S.A.* 116: 12410–12415.
44. Evrard, M., E. Wynne-Jones, C. Peng, Y. Kato, S. N. Christo, R. Fonseca, S. L. Park, T. N. Burn, M. Osman, S. Devi, et al. 2022. Sphingosine 1-phosphate receptor 5 (S1PR5) regulates the peripheral retention of tissue-resident lymphocytes. *J. Exp. Med.* 219: e20210116.
45. Benechet, A. P., M. Menon, D. Xu, T. Samji, L. Maher, T. T. Murooka, T. R. Mempel, B. S. Sheridan, F. M. Lemoine, and K. M. Khanna. 2016. T cell-intrinsic S1PR1 regulates endogenous effector T-cell egress dynamics from lymph nodes during infection. *Proc. Natl. Acad. Sci. U.S.A.* 113: 2182–2187.
46. Nansen, A., O. Marker, C. Bartholdy, and A. R. Thomsen. 2000. CCR2$^+$ and CCR5$^+$ CD8$^+$ T cells increase during viral infection and migrate to sites of infection. *Eur. J. Immunol.* 30: 1797–1806.
47. Förster, R., A. C. Davalos-Misslitz, and A. Rot. 2008. CCR7 and its ligands: balancing immunity and tolerance. *Nat. Rev. Immunol.* 8: 362–371.
48. Cunningham, C. A., E. Y. Helm, and P. J. Fink. 2018. Reinterpreting recent thymic emigrant function: defective or adaptive? *Curr. Opin. Immunol.* 51: 1–6.
49. Makaroff, L. E., D. W. Hendricks, R. E. Niec, and P. J. Fink. 2009. Postthymic maturation influences the CD8 T cell response to antigen. *Proc. Natl. Acad. Sci. U.S.A.* 106: 4799–4804.
50. June, C. H., R. S. O'Connor, O. U. Kawalekar, S. Ghassemi, and M. C. Milone. 2018. CAR T cell immunotherapy for human cancer. *Science* 359: 1361–1365.
51. Jena, B., G. Dotti, and L. J. Cooper. 2010. Redirecting T-cell specificity by introducing a tumor-specific chimeric antigen receptor. *Blood* 116: 1035–1044.
52. Eshhar, Z., T. Waks, G. Gross, and D. G. Schindler. 1993. Specific activation and targeting of cytotoxic lymphocytes through chimeric single chains consisting of antibody-binding domains and the gamma or zeta subunits of the immunoglobulin and T-cell receptors. *Proc. Natl. Acad. Sci. U.S.A* 90: 720–724.
53. Xu, N., B. Tse, L. Yang, T. C. Y. Tang, M. Haber, K. Micklethwaite, and A. Dolnikov. 2021. Priming leukemia with 5-azacytidine enhances CAR T cell therapy. *ImmunoTargets Ther.* 10: 123–140.

54. Hiwarkar, P., W. Qasim, I. Ricciardelli, K. Gilmour, S. Quezada, A. Saudemont, P. Amrolia, and P. Veys. 2015. Cord blood T cells mediate enhanced anti-tumor effects compared with adult peripheral blood T cells. *Blood* 126: 2882–2891.
55. Liang, Y., J. Shen, Q. Lan, K. Zhang, Y. Xu, M. Duah, K. Xu, and B. Pan. 2022. Blockade of PD-1/PD-L1 increases effector T cells and aggravates murine chronic graft-versus-host disease. *Int. Immunopharmacol.* 110: 109051.
56. Blank, C. U., W. N. Haining, W. Held, P. G. Hogan, A. Kallies, E. Lugli, R. C. Lynn, M. Philip, A. Rao, N. P. Restifo, et al. 2019. Defining "T cell exhaustion." *Nat. Rev. Immunol.* 19: 665–674.
57. Paley, M. A., D. C. Kroy, P. M. Odorizzi, J. B. Johnnidis, D. V. Dolfi, B. E. Barnett, E. K. Bikoff, E. J. Robertson, G. M. Lauer, S. L. Reiner, and E. J. Wherry. 2012. Progenitor and terminal subsets of $CD8^+$ T cells cooperate to contain chronic viral infection. *Science* 338: 1220–1225.